Differentiation-inducing factor 1 activates cofilin through pyridoxal phosphatase and AMP-activated protein kinase, resulting in mitochondrial fission

井上, 健

Journal of Pharmacological Sciences 152 (2023) 39–49

Contents lists available at ScienceDirect

Journal of Pharmacological Sciences

journal homepage: www.elsevier.com/locate/jphs

Full Paper

Differentiation-inducing factor 1 activates cofilin through pyridoxal phosphatase and AMP-activated protein kinase, resulting in mitochondrial fission

Takeru Inoue [a], Koichi Miura [a, *], Ruzhe Han [a], Fumi Seto-Tetsuo [a, b], Masaki Arioka [a, c], Kazunobu Igawa [d], Katsuhiko Tomooka [d], Toshiyuki Sasaguri [a]

[a] Department of Clinical Pharmacology, Faculty of Medical Sciences, Kyushu University, 812-8582 Fukuoka, Japan
[b] Department of Microbiology and Oral Infection, Infection Research, Graduate School of Biochemical Sciences, Nagasaki University, Nagasaki, 852-8588, Japan
[c] Department of Pharmacology, University of Occupational and Environmental Health, School of Medicine, Kitakyushu, Fukuoka, 807-8555, Japan
[d] Institute for Materials Chemistry and Engineering, Kyushu University, Kasuga, Japan

ARTICLE INFO

Article history:
Received 26 October 2022
Received in revised form
9 February 2023
Accepted 14 February 2023
Available online 14 March 2023

Keywords:
Differentiation-inducing factor 1
Cofilin
AMP-Activated kinase
Pyridoxal phosphatase
Mitophagy

ABSTRACT

Differentiation-inducing factor 1 (DIF-1) is a morphogen produced by *Dictyostelium discoideum* that inhibits the proliferation and migration of both *D. discoideum* and most mammalian cells. Herein, we assessed the effect of DIF-1 on mitochondria, because DIF-3, which is similar to DIF-1, reportedly localizes in the mitochondria when added exogenously, however the significance of this localization remains unclear. Cofilin is an actin depolymerization factor that is activated by dephosphorylation at Ser-3. By regulating the actin cytoskeleton, cofilin induces mitochondrial fission, the first step in mitophagy. Here, we report that DIF-1 activates cofilin and induces mitochondrial fission and mitophagy mainly using human umbilical vein endothelial cells (HUVECs). AMP-activated kinase (AMPK), a downstream molecule of DIF-1 signaling, is required for cofilin activation. Pyridoxal phosphatase (PDXP)—known to directly dephosphorylate cofilin—is also required for the effect of DIF-1 on cofilin, indicating that DIF-1 activates cofilin through AMPK and PDXP. Cofilin knockdown inhibits mitochondrial fission and decreases mitofusin 2 (Mfn2) protein levels, a hallmark of mitophagy. Taken together, these results indicate that cofilin is required for DIF-1- induced mitochondrial fission and mitophagy.

1. Introduction

Dictyostelium discoideum is an amoebozoan that exists as a unicellular or multicellular organism. When surrounding food resources are exhausted, unicellular cells differentiate into multicellular fruiting bodies consisting of prestalk and prespore regions.[1,2] Differentiation-inducing factor 1 (DIF-1) is a chlorinated polyketide morphogen produced by *D. discoideum*, which inhibits growth and migration and promotes prestalk cell differentiation.[3] DIF-1 inhibits growth and migration not only in *Dictyostelium,* but also in various types of mammalian cells, such as B16BL6, A2058s, LM8, MCF-7, and 4T1 cells.[4–6] This suggests that DIF-1 is an attractive lead compound for the development of anti-cancer drugs.

To understand how DIF-1 inhibits growth and migration, we investigated the signal transduction pathways that are activated or inactivated in response to DIF-1. Previously, we found that the mTOR/S6-kinase pathway was inhibited by DIF-1, resulting in a

Abbreviations: AMPK, AMP-activated protein kinase; BNIP3, Bcl-2/adenovirus E1B interacting protein-3; BNIP3L, Bcl-2/adenovirus E1B interacting protein-3 like; CCCP, carbonyl cyanide 3-chlorophenylhydrazone; COXIV, cytochrome oxidase subunit IV; DIF-1, differentiation-inducing factor-1; ERM, ezrin-radixin-moesin; GAPDH, glyceraldehyde-3-phosphate dehydrogenase; GSK3β, Glycogen synthase kinase 3β; HSP90, heat shock protein 90; HUVEC, human umbilical vein endothelial cell; LC3, microtubule-associated protein 1 light chain 3; Mfn2, Mitofusin 2; mTORC1, mechanistic target of rapamycin complex 1; PDXP, pyridoxal phosphatase; PINK1, PTEN-induced kinase 1; SQSTM1, sequestosome-1; STAT3, signal transducer and activator of transcription 3; SVEC, SV40-transformed murine endothelial cell line; Tim23, translocase of the inner mitochondrial membrane 23; Tom20, translocase of the outer mitochondrial membrane 20; ULK1, Unc-51 like autophagy activating kinase 1; VASP, Vasodilator-stimulated phosphoprotein.

* Corresponding author.
E-mail addresses: miura.koichi.468@m.kyushu-u.ac.jp, koichi.miura1@gmail.com (K. Miura).

Peer review under responsibility of Japanese Pharmacological Society.

https://doi.org/10.1016/j.jphs.2023.02.009

decrease in cyclin D1 expression through phosphorylation and activation of AMP-activated kinase (AMPK).[6,7] AMPK functions as an energy sensor.[8] When the AMP/ATP ratio increases, AMP allosterically binds to AMPK, resulting in the phosphorylation and activation of AMPK. AMPK then phosphorylates and inhibits raptor, a component of the mechanistic target of rapamycin complex 1 (mTORC1), leading to suppression of protein synthesis and cell proliferation.

Mitochondria are another downstream target of the AMPK pathway. When mitochondria are damaged, AMPK is activated due to the suppression of ATP production and an increase in the AMP/ATP ratio. AMPK induces mitochondrial fission via phosphorylation of mitochondrial fission factor.[9] Mitochondria are double-membrane organelles that play an essential role in cellular metabolism through ATP production.[10] When mitochondria are damaged by mitochondrial uncouplers, such as carbonyl cyanide 3-chlorophenylhydrazone (CCCP), the damaged organelles are separated from healthy ones via fission to maintain mitochondrial quality.[11,12] The damaged mitochondria are then removed by mitophagy, a selective form of mitochondrial degradation in lysosomes. Interestingly, DIF-like molecules also function as mitochondrial uncouplers and decrease the ATP/AMP ratio.[13]

Cofilin-1 (hereafter referred to as cofilin) is an actin depolymerization factor that is activated by dephosphorylation at Ser-3 by pyridoxal phosphatase (PDXP) or slingshot 1–3. Cofilin induces mitochondrial fission by regulating the actin cytoskeleton.[14]

DIF-3 is structurally related to DIF-1 and is localized in the mitochondria.[15] DIF-3 induces mitochondrial fission in HM44 cells[13]; however, the molecular mechanisms underlying this induction of mitochondrial fission remain elusive. Hence, in the present study, we evaluated whether DIF-1 induces mitochondrial fission, and assessed the associated molecular mechanisms. Taken together, we identified AMPK, HSP90, PDXP, and cofilin as factors associated with the signaling pathway underlying DIF-1-induced mitochondrial fission and mitophagy.

2. Materials and methods

2.1. Reagents and antibodies

The following reagents were employed throughout this study. Compound C (Selleck Chemicals, Houston, TX, USA), metformin (Wako-Fujifilm, Osaka, Japan), and Immobilon Forte HRP substrate (Millipore, Burlington, MA, USA). DIF-1 was synthesized as previously described.[16] Additionally, the following primary antibodies were applied: anti-GAPDH (1:1000, cat. no. ab8245, Abcam, Cambridge, UK), anti-Mfn2 (1:1000, cat. no. 12186-1-AP, Proteintech, Rosemont, IL, USA), anti-Tim23 (1:1000, cat. no. 11123-1-AP, Proteintech), anti-Tom20 (1:1000, cat. no. 11802-1-AP, Proteintech), anti-cofilin (1:1000, #5175, Cell Signaling Technology (CST), Beverly, MA, USA), anti-p-cofilin (Ser3, 1:1000, #3313, CST), anti-AMPK (1:1000, #5831, CST), anti-p-AMPK (Thr172, 1:1000, #2535, CST), anti-PDXP (1:1000, #4686, CST), anti-Ezrin/Radixin/Moesin (1:1000, #3142, CST), anti-Phospho-Ezrin (Thr567)/Radixin (Thr564)/Moesin (Thr558) (1:1000, #3726, CST), anti-talin (1:1000, #4021, CST), anti-p-talin (Ser425, 1:1000, #13589, CST), anti-VASP (Ser157, 1:1000, #3111, CST), anti-p-VASP (Ser239, 1:1000, #3114, CST), anti-VASP (1:1000, #3132, CST), anti-COXIV (1:250, #4850, CST), and anti-HA antibody (1:1000, cat. no. M180-3, MBL, Tokyo, Japan). The secondary antibodies comprised HRP-labeled anti-mouse (1:2000, #7076, CST) and anti-rabbit (1:2000, #7074, CST) IgG antibodies.

2.2. siRNAs

siRNAs targeting human cofilin (sicofilin #1) and control siRNA duplexes were purchased from Sigma-Aldrich (St. Louis, MO, USA). siRNAs targeting human cofilin (sicofilin #2), mouse PDXP, and human PDXP were purchased from Nippon Gene (Tokyo, Japan). The nucleotide sequences used for siRNAs are listed in Table 1.

2.3. Plasmids

The HSP90-HA expression vector was constructed by introducing the heat shock protein 90 (HSP90) fragment, amplified by PCR from cDNA derived from human umbilical vein endothelial cells (HUVECs, Lonza, Walkersville, MD, USA), into the *Bam*HI and *Eco*RI sites of pcDNA3-HA C.

The COXIV-Venus expression vector was constructed by introducing the COXIV fragment, amplified by PCR from pMitophagy Keima-Red mPark2 (MBL, Tokyo, Japan), which encodes COXIV, into the *Bam*HI and *Eco*RI sites of pmVenus-N1. The cofilin WT-Flag expression vector was constructed by introducing the cofilin fragment, amplified by PCR from vector IRAL025O22 (RIKEN BRC through the National Bio-Resource Project of the MEXT/AMED, Japan), which encodes human cofilin-1, into the *Bam*HI and *Eco*RI sites of pCX4 puro Flag. Two cofilin mutant expression vectors that mimic either the dephosphorylated (cofilin S3A, constitutively active) or phosphorylated (cofilin S3D, dominant-negative) form

Table 1
Nucleotide sequences used in this study.

Nucleotide sequences used to knockdown human cofilin-1	
human cofilin #1	GGAGAGCAAGAAGGAGGAU
human cofilin #2	AGCAUGAAUUGCAAGCAAA
Nucleotide sequences used to knockdown PDXP	
mouse PDXP	ACCGGUCCUUGAACUUAAU
human PDXP	CACCUCUCCUUUACAAAGA
Primers used to construct pcDNA3 HSP90-HA	
HSP90 HA F	TACCGAGCTCGGATCCGCCACCATGCCTGAGGAAGTGCAC
HSP90 HA R	GATATCTGCAGAATTCATCGACTTCTTCCATGCGA
Primers used to construct pmVenus N1 COXIV	
COXIV-Venus F	CTCAAGCTTCGAATTCGCCACCATGCTGAGCCTGCGCCAG
COXIV-Venus R	GGCGACCGGTGGATCCCACCTGGAACTGCACAGA
Primers used to construct pCX4 puro cofilinWT-Flag	
cofilinWT-Flag F	CTAGACTGCCGGATCGGAAACATGGCCTCCGGT
cofilinWT-Flag R	CCTTGTAGTCGAATTCCAAAGGCTTGCCCTCCA
Primers used for introducing point mutations into cofilin	
cofilinS3A-Flag F	GGAAACATGGCCGCCGGTGTGGCTGTCTCTGATG
cofilinS3A-Flag R	GACAGCCACACCGGCGGCCATGTTTCCGATCCG
cofilinS3D-Flag F	GGAAACATGGCCGACGGTGTGGCTGTCTCTGATG
cofilinS3D-Flag R	GACAGCCACACCGTCGGCCATGTTTCCGATCCG

were constructed by introducing point mutations into cofilin WT-Flag. The primers used are listed in Table 1.

The pcDNA3 mito-SRAI was provided by RIKEN BRC through the National Bio-Resource Project of the MEXT/AMED, Japan.[17]

2.4. Cell culture

HEK293T, MCF-7, and 4T1 cells, as well as SV40-transformed murine endothelial cell lines (SVECs) were cultured in Dulbecco's Modified Eagle Medium (Sigma-Aldrich) supplemented with 10% fetal bovine serum (FBS, Nichirei, Tokyo, Japan), 100 U/mL penicillin G (Meiji, Tokyo, Japan), and 100 μg/mL streptomycin (Meiji). HUVECs were cultured in Endothelial Cell Growth Medium 2 Kit (Takara, Shiga, Japan) at 37 °C in a 5% CO_2 atmosphere.

2.5. Transfection, RNA interference, and western blotting

Cells were seeded in 35-mm dishes (1×10^5 cells/dish). After 24 h, transient transfection of cDNA was performed using Viafect (Promega, Madison, WI, USA). The siRNA transfection was performed using Lipofectamine RNAiMAX (Invitrogen). After 24 h, the cells were lysed with 2 × SDS sample buffer (0.125 M Tris-HCl pH 6.8, 20% glycerol, 4% SDS, 10% 2-mercaptoethanol, 0.015% bromophenol blue), sonicated, and boiled. SDS-PAGE and wet transfer to polyvinylidene fluoride membranes were performed as previously described.[18] Membranes were blocked using PVDF blocking reagent (TOYOBO, Osaka, Japan) and incubated with primary antibodies diluted with Can Get Signal (TOYOBO) at 4 °C overnight. Membranes were washed with TBS-T using SNAP i.d.® 1.0 (Millipore) and incubated with HRP-labeled secondary antibodies diluted with TBS-T at room temperature for 30 min. Protein band images were obtained using Immobilon Forte and ImageQuant LAS 4010 (GE Healthcare, Chicago, IL, USA) or Amersham ImageQuant 800 (GE Healthcare). ImageJ software (NIH, Bethesda, MD, USA) was used to analyze the detected protein bands.

2.6. Immunoprecipitation

For the co-immunoprecipitation assay of HSP90 with PDXP, HEK293T cells were transfected with HA-tagged HSP90 expression vector. After 24 h, cells were lysed with lysis buffer (50 mM Tris-HCl pH 7.4, 150 mM NaCl, 5 mM EDTA, and 1% Triton X-100). Whole-cell

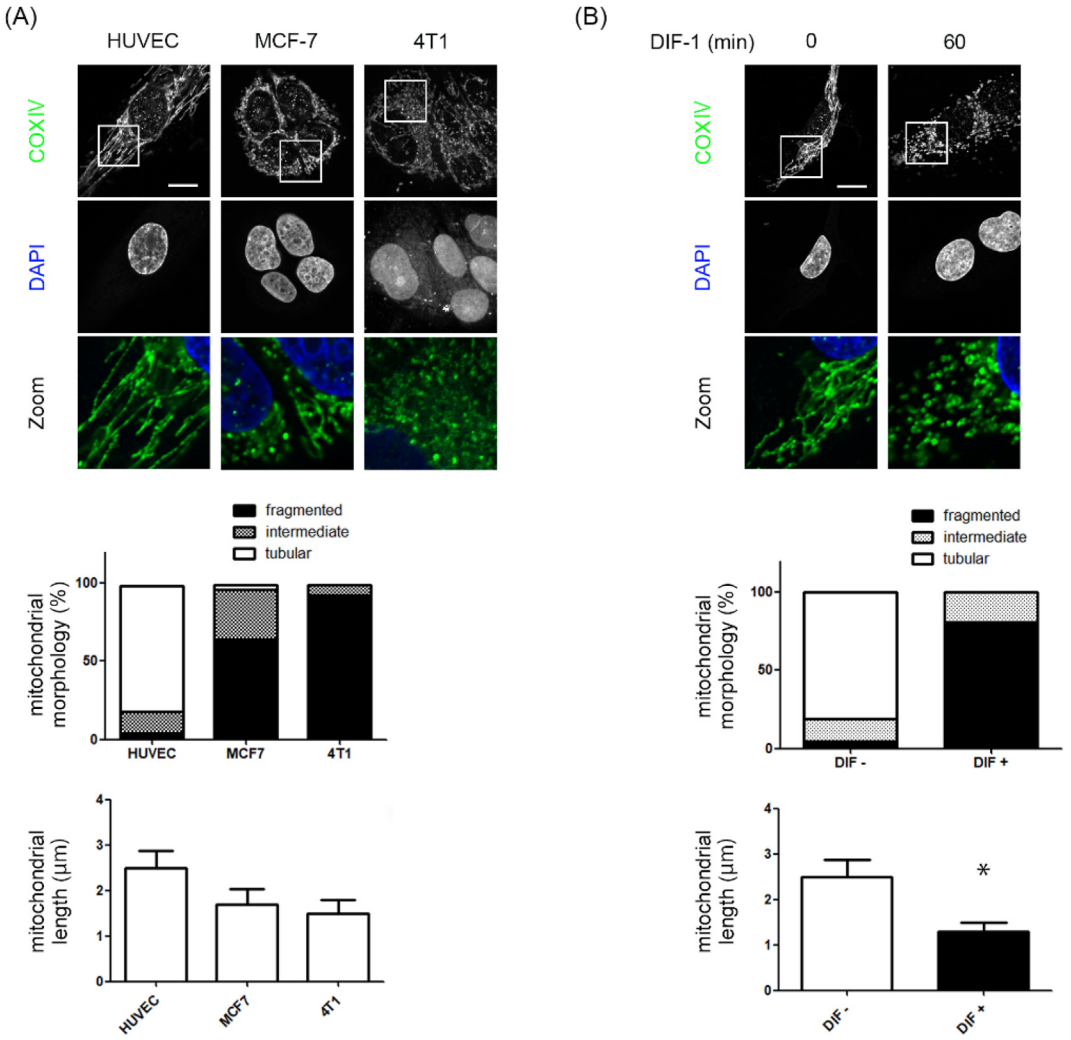

Fig. 1. DIF-1 induces mitochondrial fission in HUVECs. (A) Fluorescence images (upper), morphology (middle), and length (lower) of the mitochondria in HUVECs, MCF-7 cells, and 4T1 cells. Cells were stained with an anti-COXIV antibody (green) and DAPI (blue). Bar, 20 μm. (B) Fluorescence images (upper), morphology (middle), and length (lower) of the mitochondria in HUVECs stimulated with DIF-1. Cells were stimulated with DIF-1 (30 μM) for 60 min and stained with anti-COXIV antibody (green) and DAPI (blue). Scale bar, 20 μm.

extracts were immunoprecipitated using either monoclonal anti-HA antibody or control mouse IgG antibody coupled to Protein G Mag Sepharose (Cytiva, Tokyo, Japan) at room temperature for 1 h on a rotator. After three washes with lysis buffer, bound proteins were eluted using 2 × SDS sample buffer. The samples were analyzed using western blotting.

2.7. Immunofluorescence microscopy

Cells were grown on glass-bottom dishes, fixed with 4% paraformaldehyde, permeabilized with 0.2% Triton X-100 in Phosphate-buffered saline (PBS) for 3 min, blocked with 2% bovine serum albumin (BSA) in PBS for 1 h, incubated with primary antibodies in 2%

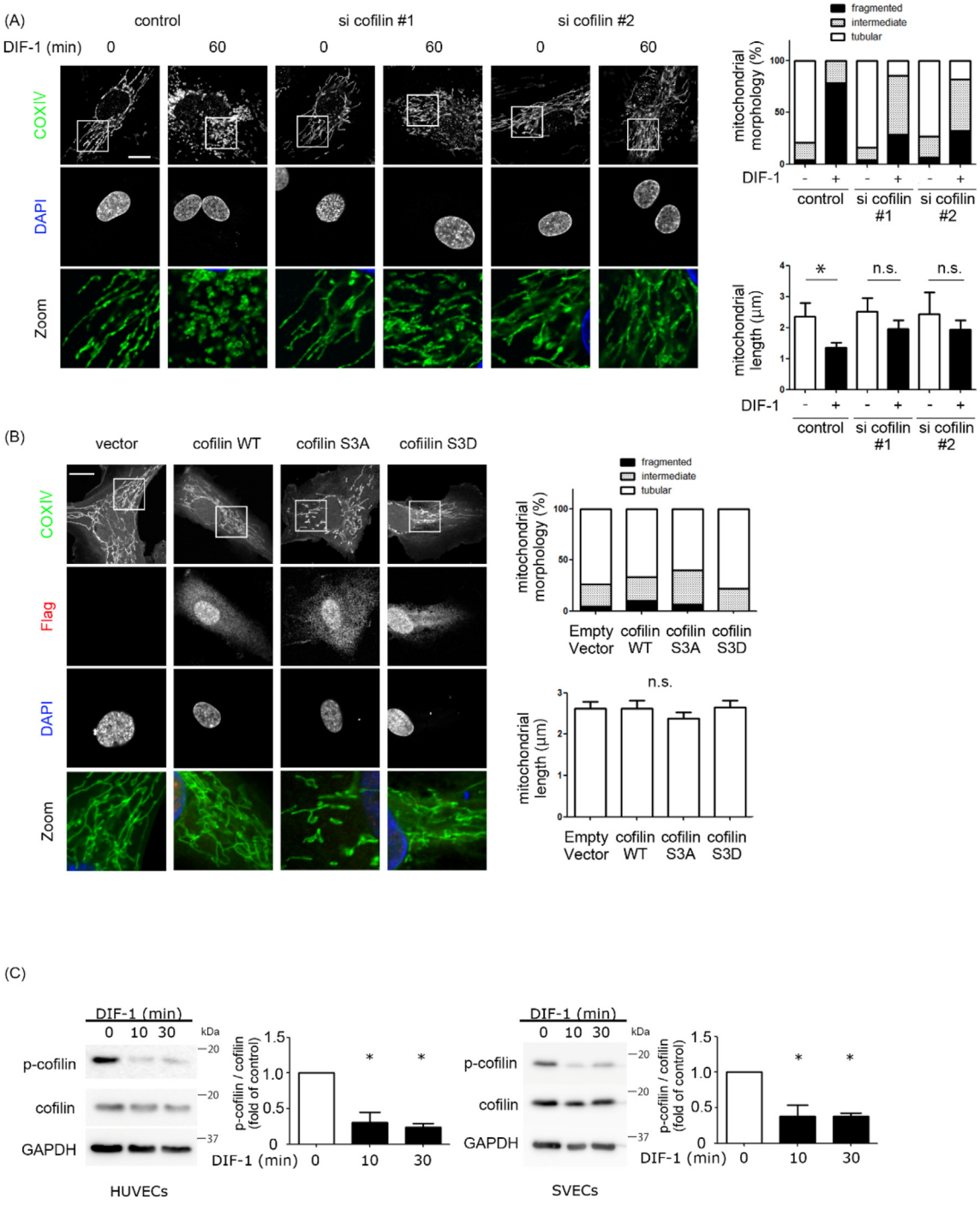

Fig. 2. DIF-1 dephosphorylates cofilin in HUVECs and SVECs. (A) Effect of cofilin knockdown on mitochondrial fission induced by DIF-1 in HUVECs. Fluorescence images (left), morphology (right upper), and length (right lower) of mitochondria in HUVECs. Cells were transfected with sicofilin or negative control for 24 h. Thereafter, cells were stimulated with DIF-1 (30 μM) for 60 min and stained with anti-COXIV antibody (green) and DAPI (blue). Scale bar, 20 μm. (B) Effect of cofilin mutants on mitochondrial fission induced by DIF-1 in HUVECs. Fluorescence images (left), morphology (right upper), and length (right lower) of mitochondria in HUVECs. Cells were co-transfected with Venus-COXIV expression vector and cofilin expression vectors as indicated. After 24 h, cells were stimulated with DIF-1 (30 μM) for 60 min and stained with anti-Flag antibody (red) and DAPI (blue). Scale bar, 20 μm. (C) Western blot analysis of HUVECs and SVECs. Cells were stimulated with DIF-1 (30 μM) for the indicated time. Blots were stained with antibodies indicated on the left. The results are presented as mean ± SD of three independent experiments.

BSA in PBS for 1 h, and then incubated with Alexa Fluor–conjugated secondary antibodies and DAPI for 1 h. Fluorescent images were acquired using a confocal microscope (LSM700; Zeiss, Oberkochen, Germany). Mitochondrial morphology was scored as previously described.[19] Briefly, we classified mitochondria into three groups: tubular, long and higher interconnectivity; intermediate, a mixture of round and shorter tubulation; and fragmented, predominantly small and round. The percentage of cells with indicated mitochondrial morphology was calculated as a percentage of the total number of transfected cells counted ($n > 10$). Mitochondrial lengths were analyzed using Metamorph software (Molecular Devices, Sunnyvale, CA, USA). TOLLES/Ypet ratio of mito-SRAI-expressing HUVECs was calculated and analyzed using ZEN2010Black (Zeiss). The mitochondrial length and morphology, as well as the ratio of mito-SRAI (TOLLES/Ypet), were determined as an average of at least 10 independent cells.

2.8. Statistical analysis

Quantitative differences among multiple groups were analyzed by one-way or two-way analysis of variance followed by Tukey's post hoc test. Differences between the two groups were analyzed by Student's unpaired *t*-test using GraphPad Prism 5.0 (GraphPad Software Inc., San Diego, CA, USA). Values are expressed as mean ± SD. Statistical significance was set at $p < 0.05$.

3. Results

3.1. DIF-1 induces mitochondrial fission in HUVECs

To observe mitochondrial fission clearly, we first visualized mitochondria in HUVECs, MCF-7 cells, and 4T1 cells using an anti-COXIV antibody. Then mitochondrial morphology and length were

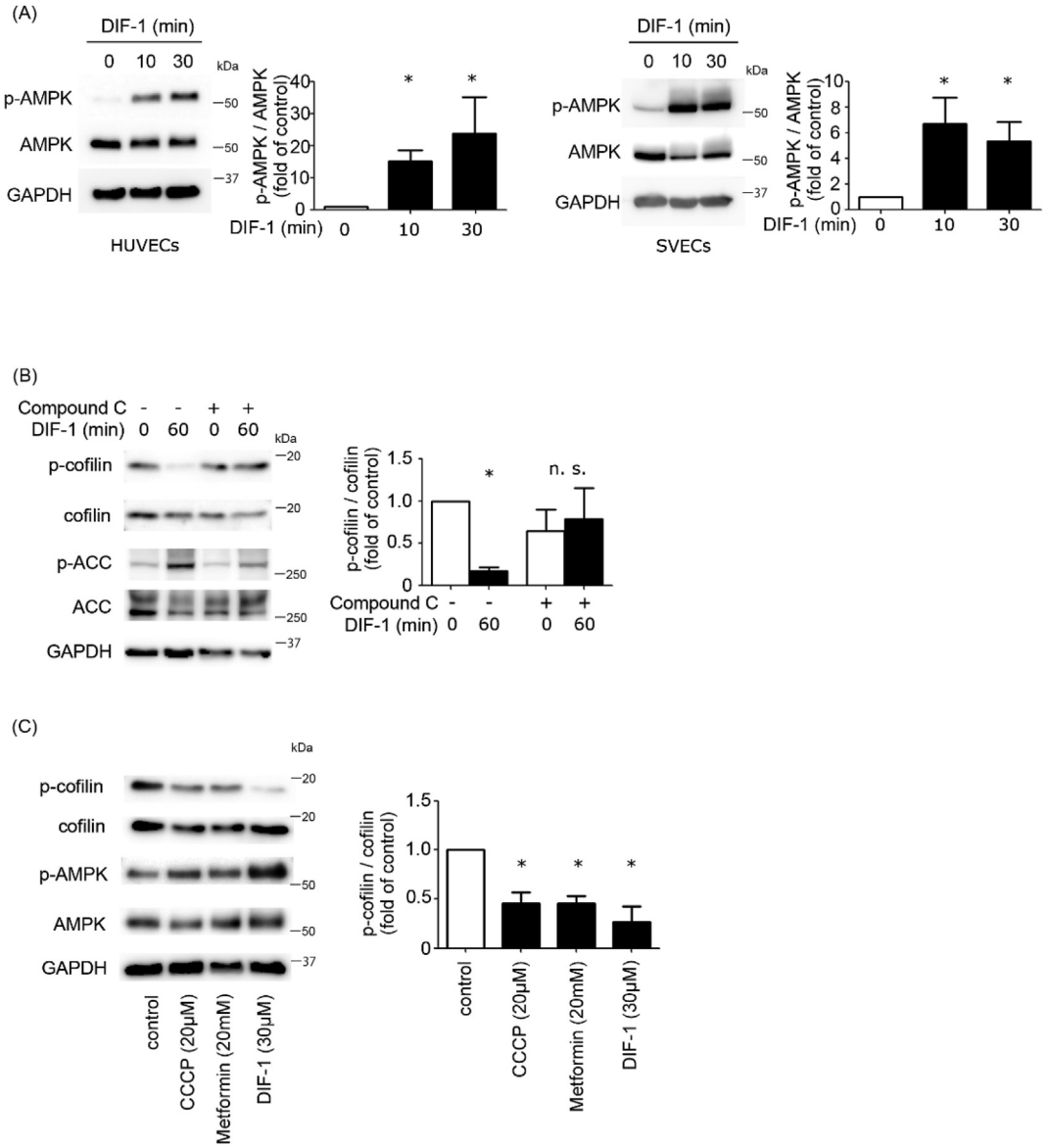

Fig. 3. AMPK is the upstream kinase of cofilin in DIF-1 signaling. (A) Western blot analysis of HUVECs (left) and SVECs (right). Cells were stimulated with DIF-1 (30 μM) for the indicated time. Blots were stained with antibodies indicated on the left. The results are presented as mean ± SD of three independent experiments. (B) Western blot analysis of HUVECs. Cells were stimulated with DIF-1 (30 μM) for 60 min with or without pretreatment of compound C (5 μM) for 24 h. Blots were stained with antibodies indicated on the left. The results are presented as mean ± SD of three independent experiments. (C) Western blot analysis of HUVECs. Cells were stimulated with DIF-1 (30 μM), Metformin (20 mM) or CCCP (20 μM) for 6 h. Blots were stained with antibodies indicated on the left. The results are presented as mean ± SD of three independent experiments.

determined. As shown in Fig. 1A, HUVECs showed the highest percentage of cells with tubular morphology and the lengthiest mitochondrial network. Therefore, we used HUVECs for subsequent experiments. Next, we examined the effect of DIF-1 on mitochondrial morphology. Similar to DIF-3, DIF-1 decreased the percentage of cells with tubular morphology and shortened the length of the mitochondrial network within 1 h (Fig. 1B), indicating that DIF-1 induces mitochondrial fission.

3.2. Cofilin is required for mitochondrial fission by DIF-1

Li et al. (2018) reported that the knockdown of cofilin inhibits mitochondrial fission by CCCP, while overexpression of wild-type cofilin promotes mitochondrial fission.[14] We assessed whether cofilin is required for mitochondrial fission induced by DIF-1. As shown in Fig. 2A, cofilin knockdown attenuated mitochondrial fission induced by DIF-1.

We also evaluated the effect of active (S3A) and inactive (S3D) cofilin mutants on mitochondrial fission induced by DIF-1. As shown in Fig. 2B, overexpression of cofilin or its mutants alone did not change the mitochondrial morphology or shorten the mitochondrial length. Hence, DIF-1 and cofilin together induce a significant change in mitochondrial morphology and length, but cofilin activation alone is insufficient to alter these mitochondrial characteristics.

3.3. DIF-1 dephosphorylates cofilin in endothelial cells

We assessed whether DIF-1 dephosphorylates and activates cofilin. We observed significant cofilin dephosphorylation in HUVECs and SVECs, a mouse immortalized endothelial cell line (Fig. 2C).

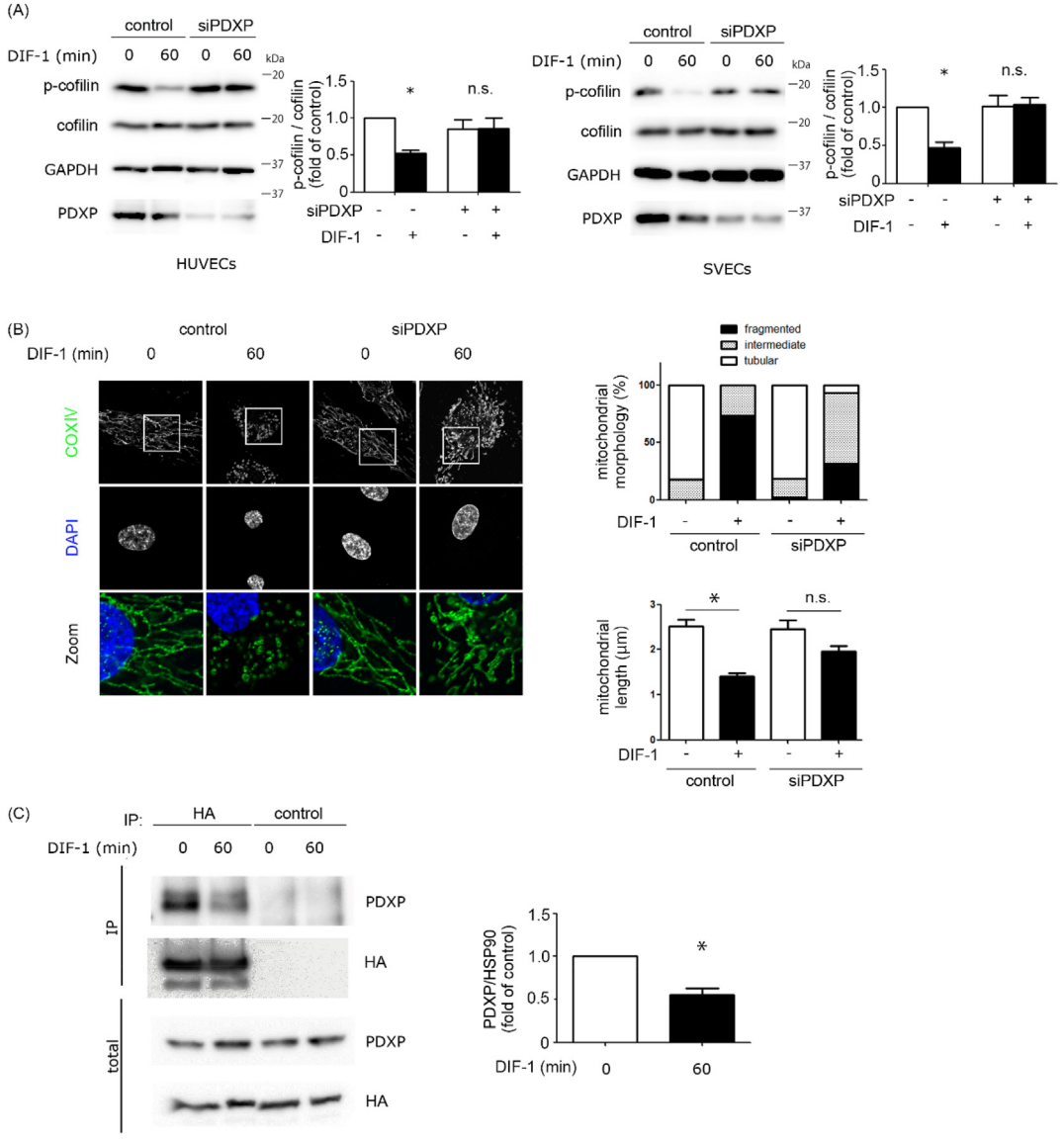

Fig. 4. PDXP dephosphorylates cofilin in DIF-1 signaling. (A) Western blot analysis of HUVECs (left) and SVECs (right). Cells were transfected with siPDXP or negative control. After 24 h, cells were stimulated with DIF-1 (30 μM) for 60 min and stained with antibodies indicated on the left. The results are presented as mean ± SD of three independent experiments. (B) Effect of PDXP knockdown on mitochondrial fission induced by DIF-1 in HUVECs. Fluorescence images (left), morphology (right upper), and length (right lower) of mitochondria in HUVECs. Cells were transfected with siPDXP or negative control for 24 h. Thereafter, cells were treated with DIF-1 (30 μM) for 60 min and stained with anti-COXIV antibody (green) and DAPI (blue). Scale bar, 20 μm. (C) Effect of DIF-1 on the interaction between HSP90 and PDXP. HEK293T cells were transfected with HSP90-HA expressing vector. After 24 h, cells were stimulated with DIF-1 (30 μM) for 30 min. Immunoprecipitation was performed using anti-HA antibody or control mouse IgG antibody conjugated with Protein G magnetic beads (left). The ratio of PDXP/HA-HSP90 is presented as mean ± SD of three independent experiments (right).

3.4. AMPK is the upstream kinase of cofilin in DIF-1 signaling

Next, we sought to identify the upstream molecules involved in the dephosphorylation and activation of cofilin by DIF-1. We focused on AMPK as it is activated by DIF-1 in MCF-7 and 4T1 cells[6] and is involved in mitochondrial fission induction and mitophagy in C2C12 cells.[20] In addition to HUVECs, we also tested SVECs, mouse endothelial cells, to confirm whether DIF-1 could induce cofilin dephosphorylation in cells of other species. As expected, AMPK was phosphorylated and activated by DIF-1 in HUVECs and SVECs (Fig. 3A). We then investigated the effect of compound C, an AMPK inhibitor, on the dephosphorylation of cofilin by DIF-1. As

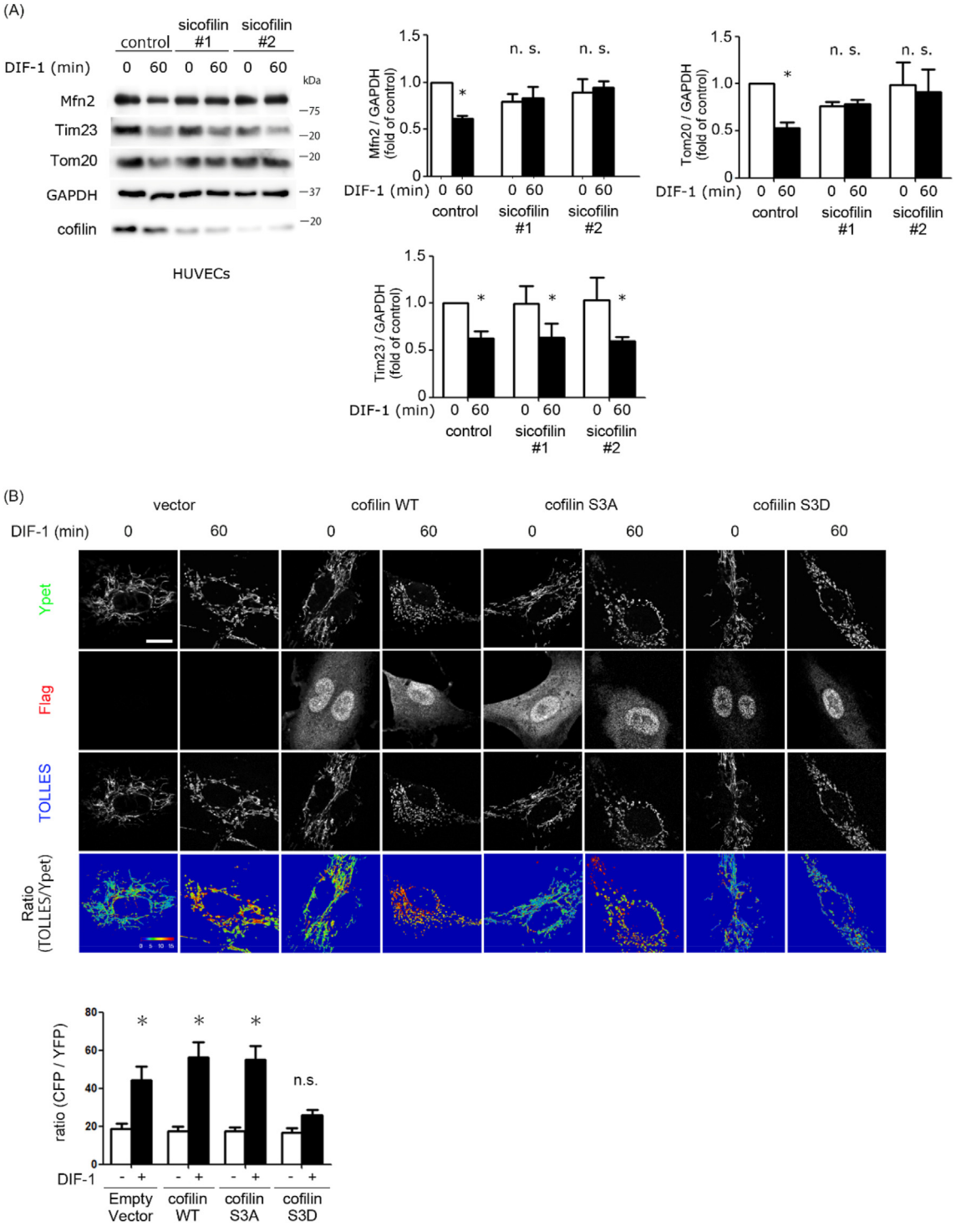

Fig. 5. Cofilin induces mitochondrial fission. (A) Western blot and quantitative analysis of HUVECs. Cells were transfected with sicofilin or negative control for 24 h. Thereafter, cells were stimulated with DIF-1 (30 μM) for the indicated time. Blots were stained with antibodies indicated on the left. The results are presented as mean ± SD of three independent experiments. (B) Fluorescence and ratio (TOLLES/Ypet) images (upper) and quantitative analysis of the ratio images (lower) of HUVECs stimulated by DIF-1. Cells were co-transfected with mito-SRAI expression vector and cofilin expression vectors as indicated. After 24 h, cells were stimulated with DIF-1 (30 μM) for 60 min and stained with anti-Flag antibody (red), followed by Alexa594 anti mouse IgG antibody. Ratio images were obtained using LSM700 confocal microscopy. Scale bar, 20 μm.

shown in Fig. 3B, Compound C strongly inhibited DIF-1-induced dephosphorylation of cofilin and phosphorylation of acetyl CoA carboxylase (ACC), a major substrate of AMPK, in HUVECs. These results indicate that AMPK is required for cofilin activation and mitochondrial fission by DIF-1. CCCP and metformin are well-known AMPK activators.[21,22] Moreover, CCCP and metformin were reported to induce mitochondrial fission.[14,23] Consistently, these compounds also dephosphorylated cofilin, similar to DIF-1 (Fig. 3C), indicating that cofilin is a common target of AMPK activators.

3.5. PDXP dephosphorylates cofilin in DIF-1 signaling

Pyridoxal phosphatase (PDXP), also known as chronophin, is activated by ATP depletion[24] and directly dephosphorylates cofilin.[25] When PDXP was knocked down, cofilin dephosphorylation by DIF-1 was inhibited in both HUVECs and SVECs (Fig. 4A), indicating that PDXP is required for cofilin dephosphorylation induced by DIF-1.

We also evaluated the effect of PDXP knockdown on DIF-1-induced morphological change of mitochondria. PDXP knockdown inhibited mitochondrial fission (Fig. 4B), suggesting that DIF-1 induces mitochondrial fission via PDXP, followed by cofilin dephosphorylation and activation.

Under normal conditions, PDXP is inactivated by its association with HSP90.[26] Attenuation of the association between PDXP and HSP90 induces PDXP activation, resulting in cofilin dephosphorylation and activation. To verify the attenuation of the association by DIF-1, a co-immunoprecipitation assay was performed. As shown in Fig. 4C, the association between endogenous PDXP and HSP90-HA overexpression was suppressed by DIF-1. These results suggest that DIF-1 dephosphorylates cofilin by inhibiting the association between PDXP and HSP90.

3.6. DIF-1 induces mitophagy via cofilin activation

The levels of several mitochondrial proteins, including Mfn2, Tim23, and Tom20 are reported to be reduced during mitophagy.[27,28] To test whether DIF-1 induces mitophagy, we investigated mitochondrial protein levels including Mfn2, Tim23, and Tom20 before and after DIF-1 treatment. As shown in Fig. 5A, DIF-1 reduced protein levels of Mfn2, Tim23, and Tom20. The decrease in the levels of Mfn2 and Tom20, but not Tim23, was blocked by cofilin knockdown. These results also support the notion that DIF-1 induces mitophagy through cofilin activation.

We also tested the effect of DIF-1 on mitophagy using mito-SRAI, which is a recently developed mitophagy indicator.[17] Mito-SRAI has a tandem construct coupled with TOLLES and Ypet. After lysosomal delivery, the complete degradation of Ypet results in the dequenching of TOLLES, producing a high TOLLES/Ypet ratio.[17] DIF-1 increased the mito-SRAI ratio (TOLLES/Ypet). This implies that DIF-1 induces mitophagy following mitochondrial fission (Fig. 5B).

We then tested the effect of overexpression of wildtype cofilin and its active or inactive mutants on mitophagy. As shown in Fig. 5B, the inactive mutant of cofilin (S3D) inhibited the increase of mito-SRAI ratio that was induced by DIF-1. Altogether, these data suggest that cofilin activity is required for mitophagy induction by DIF-1.

3.7. Effects of DIF-1 treatment on phosphorylation of other actin regulators

Finally, we tested whether DIF-1 regulates other actin regulators, including VASP, ERM, and talin, in addition to cofilin. As shown in Fig. 6A, a clear change in the phosphorylation status by DIF-1 was only observed in cofilin. Hence, DIF-1 specifically regulates cofilin among actin regulators.

4. Discussion

DIF-1 regulates the phosphorylation of many signaling molecules, including AMPK, S6-kinase, raptor, ACC, ULK1, GSK3β, and STAT3.[6,29] In the present study, DIF-1 dephosphorylated and activated cofilin via AMPK activation, leading to mitochondrial fission and mitophagy.

Mitochondrial fission, followed by mitophagy, eliminates dysfunctional or damaged mitochondria by engulfing mitochondria and degrading into lysosomes. In general, this process is involved in mitochondrial turnover to keep mitochondrial quality for maintaining cell homeostasis.[9,30] Indeed, dysfunctional mitophagy has been implicated in several diseases, such as

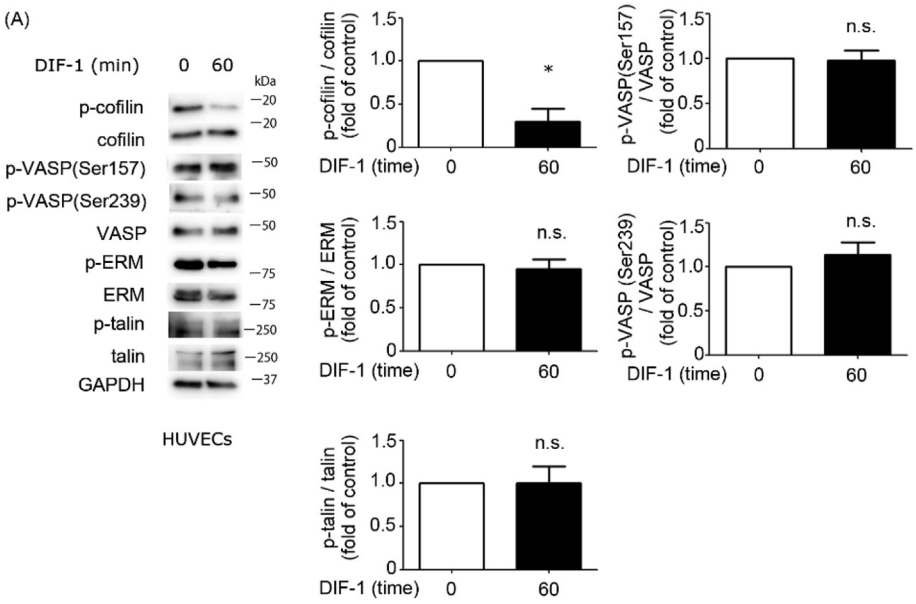

Fig. 6. DIF-1 specifically regulates cofilin among actin regulators. (A) Western blot analysis of HUVECs. Cells were stimulated with DIF-1 (30 μM) for the indicated time. Blots were stained with antibodies indicated on the left. The results are presented as mean ± SD of three independent experiments.

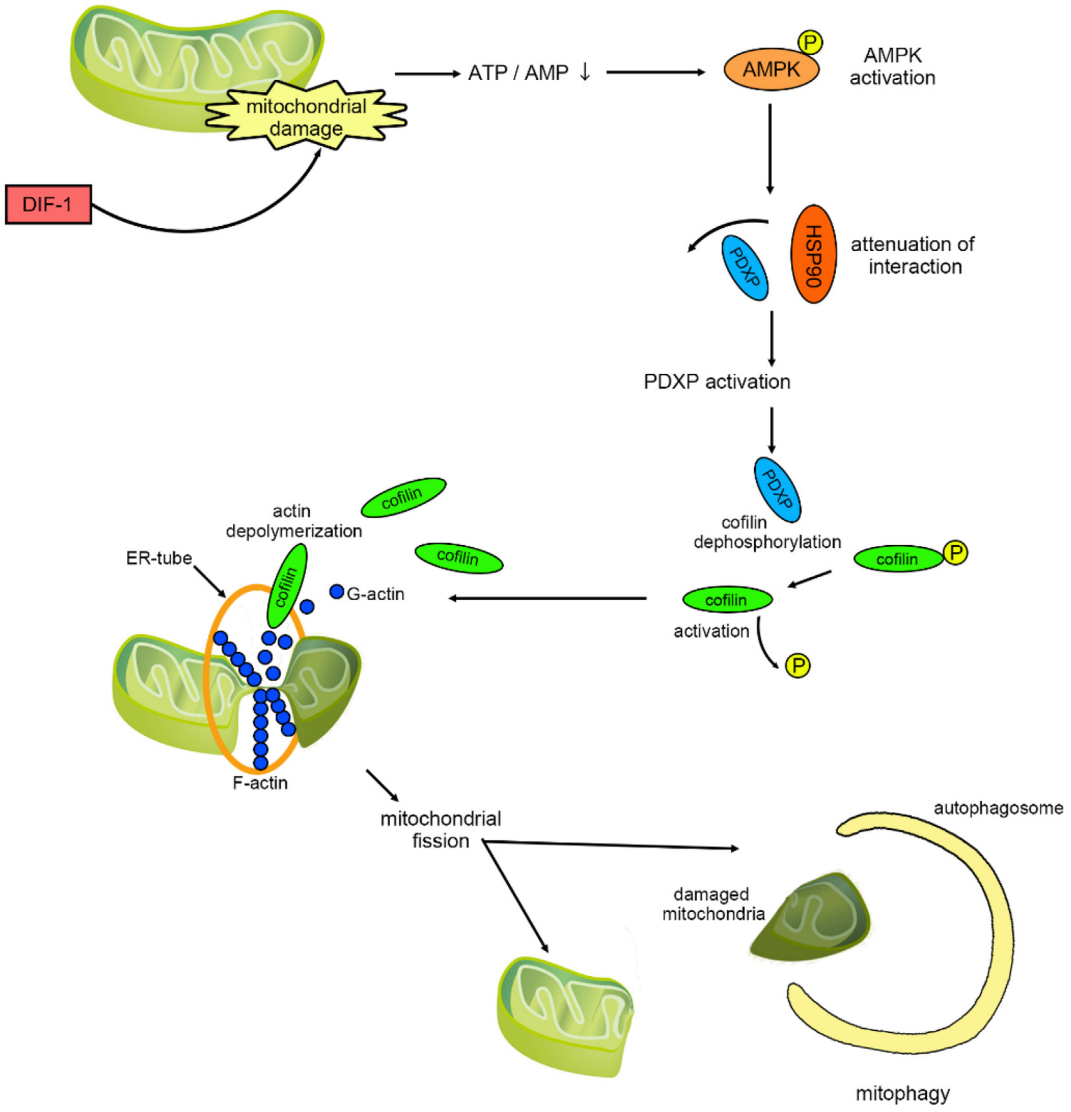

Fig. 7. Schematic representation of possible molecular signaling involved in mitochondrial fission induced by DIF-1. Previous studies reported that DIF-1 directly binds to and damages mitochondria, resulting in a decrease of intracellular ATP/AMP ratio and AMPK activation. In this study, we found that DIF-1 activates cofilin, resulting in mitochondrial fission and mitophagy. AMPK and PDXP are required for the activation of cofilin. Attenuation of the interaction between PDXP and HSP90 by DIF-1 activates PDXP. Then activated PDXP dephosphorylates and activates cofilin. Activated cofilin is known to translocated to the mitochondrial fission site and depolymerizes F-actin, leading to the segregation of the fission complex.

Alzheimer's disease, cardiomyopathy as well as other cardiac disorders, and steatohepatitis.[31–33]

In cancer, mitophagy can positively or negatively regulates cell homeostasis. For example, enhanced mitophagy contributes to cisplatin resistance in cancer cells.[34] However, excessive mitophagy reduces total mitochondria and energy production, which leads to cell death.[35] Furthermore, several proteins, such as parkin, BNIP3, BNIP3L, and p62/SQSTM1, which govern mitophagy, are silenced or downregulated in human cancer cells.[36,37] Notably, the anti-leukemic effect of DIF-3 is mediated by mitochondrial fission without caspase-dependent cell death.[38] Therefore, mitophagy can either support cancer cell survival or promote cell death.

AMPK becomes activated when mitochondria are damaged by mitochondrial toxins, such as rotenone or CCCP.[20,39] DIF-1 may also damage mitochondria, leading to AMPK activation and mitochondrial fission.

Previously, we identified mitochondrial malate dehydrogenase 2 (MDH2) as a direct binding protein for DIF-1. MDH2 is a component of the TCA cycle and is involved in ATP production. We also found that DIF-1 inhibits the enzymatic activity of MDH2 *in vitro* and reduces cellular ATP levels.[40] Hence, inhibition of MDH2 by DIF-1, followed by ATP depletion, may activate AMPK.

We found that PDXP is required for cofilin dephosphorylation. Furthermore, DIF-1 attenuated the interaction between PDXP and HSP90, which is required for PDXP activation. Intriguingly, an increase in the AMP/ATP ratio suppresses the association between HSP90 and PDXP.[24] This strongly suggests that AMPK activation is involved in the dissociation between HSP90 and PDXP. Moreover, HSP90 interacts with AMPK and promotes the phosphorylation of ACC, which is downstream of AMPK.[41] Hence, DIF-1 may enhance the HSP90-AMPK interaction, resulting in inhibition of the HSP90-PDXP association.

In this study, we focused on the effects of DIF-1 on mitochondrial fission specifically in HUVECs as these cells exhibit a clear mitochondria fiber structure. Although we confirmed DIF-1 induces mitochondrial fission and mitophagy, subsequent studies with

different cancer cell lines are required to determine if DIF-1 represents a potential therapeutic agent for various cancer types.

In conclusion, we identified AMPK, HSP90, PDXP, and cofilin as new components of the DIF-1 signaling pathway, leading to mitochondrial fission and mitophagy (Fig. 7). In this study, we used HUVECs as these cells exhibit a clear mitochondria fiber structure. However, further studies are required to determine whether DIF-1 also induce mitochondrial fission and mitophagy in cancer cells, which may advance the understanding of the anti-tumor effect of DIF-1.

Author contributions

Takeru Inoue: Investigation, Validation, Visualization, Writing-original draft, Writing-review & editing. Koichi Miura: Conceptualization, Funding, Investigation, Project administration, Validation, Visualization, Writing-review & editing. Ruzhe Han: Investigation, Validation, Visualization. Fumi Seto-Tetsuo: Conceptualization, Writing-review & editing. Masaki Arioka: Conceptualization, Funding, Writing-review & editing. Kazunobu Igawa: Resources. Katsuhiko Tomooka: Resources. Toshiyuki Sasaguri: Conceptualization, Funding acquisition, Resources, Supervision, Writing-review & editing.

Funding

This work was supported by the Ministry of Education, Science, Sports, and Culture of Japan (Grant Numbers: JP17K15581, JP20K07292, and JP20K22709), Fukuoka Foundation for Sound Health Cancer Research Fund, and Kaibara Morikazu Medical Science Promotion Foundation.

Conflict of interest

The authors indicated no potential conflict of interest.

Acknowledgments

We thank F. Shiraishi (Graduate School of Medical Sciences, Kyushu University) for administrative support. We appreciate the technical support provided by the Research Support Center at the Graduate School of Medical Sciences of Kyushu University. We would also like to thank Editage (www.editage.com) for English language editing.

References

1. Thompson CR, Kay RR. The role of DIF-1 signaling in Dictyostelium development. *Mol Cell*. 2000;6(6):1509–1514. https://doi.org/10.1016/s1097-2765(00)00147-7.
2. Gokan N, Kikuchi H, Nakamura K, Oshima Y, Hosaka K, Kubohara Y. Structural requirements of Dictyostelium differentiation-inducing factors for their stalk-cell-inducing activity in Dictyostelium cells and anti-proliferative activity in K562 human leukemic cells. *Biochem Pharmacol*. 2005;70(5):676–685. https://doi.org/10.1016/j.bcp.2005.06.002.
3. Berks M, Kay RR. Combinatorial control of cell differentiation by cAMP and DIF-1 during development of Dictyostelium discoideum. *Development*. 1990;110(3):977–984.
4. Arioka M, Takahashi-Yanaga F, Kubo M, Igawa K, Tomooka K, Sasaguri T. Anti-tumor effects of differentiation-inducing factor-1 in malignant melanoma: GSK-3-mediated inhibition of cell proliferation and GSK-3-independent suppression of cell migration and invasion. *Biochem Pharmacol*. 2017;138:31–48. https://doi.org/10.1016/j.bcp.2017.05.004.
5. Kubohara Y, Komachi M, Homma Y, Kikuchi H, Oshima Y. Derivatives of Dictyostelium differentiation-inducing factors inhibit lysophosphatidic acid-stimulated migration of murine osteosarcoma LM8 cells. *Biochem Biophys Res Commun*. 2015;463(4):800–805. https://doi.org/10.1016/j.bbrc.2015.06.016.
6. Seto-Tetsuo F, Arioka M, Miura K, et al. DIF-1 inhibits growth and metastasis of triple-negative breast cancer through AMPK-mediated inhibition of the mTORC1-S6K signaling pathway. *Oncogene*. 2021;40(37):5579–5589. https://doi.org/10.1038/s41388-021-01958-4.
7. Tetsuo F, Arioka M, Miura K, et al. Differentiation-inducing factor-1 suppresses cyclin D1-induced cell proliferation of MCF-7 breast cancer cells by inhibiting S6K-mediated signal transducer and activator of transcription 3 synthesis. *Cancer Sci*. 2019;110(12):3761–3772. https://doi.org/10.1111/cas.14204.
8. Gwinn DM, Shackelford DB, Egan DF, et al. AMPK phosphorylation of raptor mediates a metabolic checkpoint. *Mol Cell*. 2008;30(2):214–226. https://doi.org/10.1016/j.molcel.2008.03.003.
9. Choubey V, Zeb A, Kaasik A. Molecular mechanisms and regulation of mammalian mitophagy. *Cells*. 2021;11(1). https://doi.org/10.3390/cells11010038.
10. Pickles S, Vigié P, Youle RJ. Mitophagy and quality control mechanisms in mitochondrial maintenance. *Curr Biol*. 2018;28(4):R170–R185. https://doi.org/10.1016/j.cub.2018.01.004.
11. Park YS, Choi SE, Koh HC. PGAM5 regulates PINK1/Parkin-mediated mitophagy via DRP1 in CCCP-induced mitochondrial dysfunction. *Toxicol Lett. Mar 01*. 2018;284:120–128. https://doi.org/10.1016/j.toxlet.2017.12.004.
12. Xian H, Liou YC. Functions of outer mitochondrial membrane proteins: mediating the crosstalk between mitochondrial dynamics and mitophagy. *Cell Death Differ. 03*. 2021;28(3):827–842. https://doi.org/10.1038/s41418-020-00657-z.
13. Kubohara Y, Kikuchi H, Nguyen VH, Kuwayama H, Oshima Y. Evidence that differentiation-inducing factor-1 controls chemotaxis and cell differentiation, at least in part, via mitochondria in D. discoideum. *Biol Open.*. 2017;6(6):741–751 https://doi.org/10.1242/bio.021345.
14. Li GB, Zhang HW, Fu RQ, et al. Mitochondrial fission and mitophagy depend on cofilin-mediated actin depolymerization activity at the mitochondrial fission site. *Oncogene*. 2018;37(11):1485–1502. https://doi.org/10.1038/s41388-017-0064-4.
15. Kubohara Y, Kikuchi H, Matsuo Y, Oshima Y, Homma Y. Properties of a non-bioactive fluorescent derivative of differentiation-inducing factor-3, an anti-tumor agent found in Dictyostelium discoideum. *Biol Open*. 2014;3(4):289–296. https://doi.org/10.1242/bio.20146585.
16. Morris HR, Taylor GW, Masento MS, Jermyn KA, Kay RR. Chemical structure of the morphogen differentiation inducing factor from Dictyostelium discoideum. *Nature*. 1987;328(6133):811–814. https://doi.org/10.1038/328811a0.
17. Katayama H, Hama H, Nagasawa K, et al. Visualizing and modulating mitophagy for therapeutic studies of neurodegeneration. *Cell*. 2020;181(5):1176–1187.e16. https://doi.org/10.1016/j.cell.2020.04.025.
18. Suzukawa K, Miura K, Mitsushita J, et al. Nerve growth factor-induced neuronal differentiation requires generation of Rac1-regulated reactive oxygen species. *J Biol Chem*. 2000;275(18):13175–13178. https://doi.org/10.1074/jbc.275.18.13175.
19. Rambold AS, Kostelecky B, Elia N, Lippincott-Schwartz J. Tubular network formation protects mitochondria from autophagosomal degradation during nutrient starvation. *Proc Natl Acad Sci U S A*. 2011;108(25):10190–10195. https://doi.org/10.1073/pnas.1107402108.
20. Seabright AP, Fine NHF, Barlow JP, et al. AMPK activation induces mitophagy and promotes mitochondrial fission while activating TBK1 in a PINK1-Parkin independent manner. *FASEB J*. 2020;34(5):6284–6301. https://doi.org/10.1096/fj.201903051R.
21. Zhou X, Kuang Y, Liang S, Wang L. Metformin inhibits cell proliferation in SKM-1 cells via AMPK-mediated cell cycle arrest. *J Pharmacol Sci*. 2019;141(4):146–152. https://doi.org/10.1016/j.jphs.2019.10.003.
22. Koncha RR, Ramachandran G, Sepuri NBV, Ramaiah KVA. CCCP-induced mitochondrial dysfunction - characterization and analysis of integrated stress response to cellular signaling and homeostasis. *FEBS J*. 2021;288(19):5737–5754. https://doi.org/10.1111/febs.15868.
23. Wang Y, An H, Liu T, et al. Metformin improves mitochondrial respiratory activity through activation of AMPK. *Cell Rep*. 2019;29(6):1511–1523.e5. https://doi.org/10.1016/j.celrep.2019.09.070.
24. Huang TY, Minamide LS, Bamburg JR, Bokoch GM. Chronophin mediates an ATP-sensing mechanism for cofilin dephosphorylation and neuronal cofilin-actin rod formation. *Dev Cell*. 2008;15(5):691–703. https://doi.org/10.1016/j.devcel.2008.09.017.
25. Gohla A, Birkenfeld J, Bokoch GM. Chronophin, a novel HAD-type serine protein phosphatase, regulates cofilin-dependent actin dynamics. *Nat Cell Biol*. 2005;7(1):21–29. https://doi.org/10.1038/ncb1201.
26. Shin EJ, Choi HK, Sung MJ, et al. Anti-tumour effects of beta-sitosterol are mediated by AMPK/PTEN/HSP90 axis in AGS human gastric adenocarcinoma cells and xenograft mouse models. *Biochem Pharmacol*. 2018;152:60–70. https://doi.org/10.1016/j.bcp.2018.03.010.
27. Benischke AS, Vasanth S, Miyai T, et al. Activation of mitophagy leads to decline in Mfn2 and loss of mitochondrial mass in Fuchs endothelial corneal dystrophy. *Sci Rep*. 2017;7(1):6656. https://doi.org/10.1038/s41598-017-06523-2.
28. Cen X, Chen Y, Xu X, et al. Pharmacological targeting of MCL-1 promotes mitophagy and improves disease pathologies in an Alzheimer's disease mouse model. *Nat Commun*. 2020;11(1):5731. https://doi.org/10.1038/s41467-020-19547-6.
29. Takahashi-Yanaga F, Yoshihara T, Jingushi K, et al. DIF-1 inhibits tumor growth in vivo reducing phosphorylation of GSK-3β and expressions of cyclin D1 and TCF7L2 in cancer model mice. *Biochem Pharmacol*. 2014;89(3):340–348. https://doi.org/10.1016/j.bcp.2014.03.006.
30. Mailloux RJ. Mitochondrial antioxidants and the maintenance of cellular hydrogen peroxide levels. *Oxid Med Cell Longev*. 2018;2018, 7857251. https://doi.org/10.1155/2018/7857251.

31. Song M, Zhao X, Song F. Aging-dependent mitophagy dysfunction in alzheimer's disease. *Mol Neurobiol. May*. 2021;58(5):2362–2378. https://doi.org/10.1007/s12035-020-02248-y.
32. Dutta D, Calvani R, Bernabei R, Leeuwenburgh C, Marzetti E. Contribution of impaired mitochondrial autophagy to cardiac aging: mechanisms and therapeutic opportunities. *Circ Res*. 2012;110(8):1125–1138. https://doi.org/10.1161/CIRCRESAHA.111.246108.
33. Glick D, Zhang W, Beaton M, et al. BNip3 regulates mitochondrial function and lipid metabolism in the liver. *Mol Cell Biol*. 2012;32(13):2570–2584. https://doi.org/10.1128/MCB.00167-12.
34. Villa E, Proïcs E, Rubio-Patiño C, et al. Parkin-independent mitophagy controls chemotherapeutic response in cancer cells. *Cell Rep*. 2017;20(12):2846–2859. https://doi.org/10.1016/j.celrep.2017.08.087.
35. Panigrahi DP, Praharaj PP, Bhol CS, et al. The emerging, multifaceted role of mitophagy in cancer and cancer therapeutics. *Semin Cancer Biol*. 2020;66:45–58. https://doi.org/10.1016/j.semcancer.2019.07.015.
36. Chourasia AH, Boland ML, Macleod KF. Mitophagy and cancer. *Cancer Metab*. 2015;3:4. https://doi.org/10.1186/s40170-015-0130-8.
37. Drake LE, Springer MZ, Poole LP, Kim CJ, Macleod KF. Expanding perspectives on the significance of mitophagy in cancer. *Semin Cancer Biol*. 2017;47:110–124. https://doi.org/10.1016/j.semcancer.2017.04.008.
38. Dubois A, Ginet C, Furstoss N, et al. Differentiation inducing factor 3 mediates its anti-leukemic effect through ROS-dependent DRP1-mediated mitochondrial fission and induction of caspase-independent cell death. *Oncotarget*. 2016;7(18):26120–26136. https://doi.org/10.18632/oncotarget.8319.
39. Hayashi T, Hirshman MF, Fujii N, Habinowski SA, Witters LA, Goodyear LJ. Metabolic stress and altered glucose transport: activation of AMP-activated protein kinase as a unifying coupling mechanism. *Diabetes*. 2000;49(4):527–531. https://doi.org/10.2337/diabetes.49.4.527.
40. Matsuda T, Takahashi-Yanaga F, Yoshihara T, et al. Dictyostelium differentiation-inducing factor-1 binds to mitochondrial malate dehydrogenase and inhibits its activity. *J Pharmacol Sci*. 2010;112(3):320–326. https://doi.org/10.1254/jphs.09348fp.
41. Zhang L, Yi Y, Guo Q, et al. Hsp90 interacts with AMPK and mediates acetyl-CoA carboxylase phosphorylation. *Cell Signal*. 2012;24(4):859–865. https://doi.org/10.1016/j.cellsig.2011.12.001.